Temperature Dependence of the Band Gap of Semiconducting Carbon Nanotubes

Rodrigo B. Capaz,[1,2,3] Catalin D. Spataru,[2,3] Paul Tangney,[2,3] Marvin L. Cohen,[2,3] and Steven G. Louie[2,3]

[1]*Instituto de Física, Universidade Federal do Rio de Janeiro, Caixa Postal 68528, Rio de Janeiro, RJ 21941-972, Brazil*

[2]*Department of Physics, University of California at Berkeley, Berkeley, California 94720, USA*

[3]*Materials Science Division, Lawrence Berkeley National Laboratory, Berkeley, California 94720, USA*

(Received 22 June 2004; published 25 January 2005)

The temperature dependence of the band gap of semiconducting single-wall carbon nanotubes (SWNTs) is calculated by direct evaluation of electron-phonon couplings within a "frozen-phonon" scheme. An interesting diameter and chirality dependence of $E_g(T)$ is obtained, including nonmonotonic behavior for certain tubes and distinct "family" behavior. These results are traced to a strong and complex coupling between band-edge states and the lowest-energy optical phonon modes in SWNTs. The $E_g(T)$ curves are modeled by an analytic function with diameter- and chirality-dependent parameters; these provide a valuable guide for systematic estimates of $E_g(T)$ for any given SWNT. The magnitudes of the temperature shifts at 300 K are smaller than 12 meV and should not affect (n, m) assignments based on optical measurements.

DOI: 10.1103/PhysRevLett.94.036801 PACS numbers: 73.22.–f, 63.22.+m, 71.38.–k

The temperature dependence of the band gap (E_g) is one of the fundamental signatures of a semiconductor, providing important insight into the nature and strength of electron-phonon (e-p) interactions. The first measurements of $E_g(T)$ date from the dawn of the semiconductor era [1]. Typically, $E_g(T)$ curves show a monotonic decrease with temperature that is nonlinear at low T and linear at sufficiently high T [2,3].

Semiconducting carbon nanotubes are relatively novel semiconductor materials [4], with a variety of potential applications. Despite intensive research since their discovery, it has only recently become possible to perform measurements of the optical gap in individual single-wall carbon nanotubes (SWNTs) [5–10]. Such measurements, combined with information from vibrational spectroscopy, provide a route to (n, m) assignment of SWNTs [5,8,9]. Understanding $E_g(T)$ for nanotubes is extremely important in this context, since experiments are usually performed at room temperature and (n, m) assignments are often guided by comparisons between observed optical transition patterns and the corresponding predictions from calculations at $T = 0$ K. Moreover, the $E_g(T)$ signature could provide extra information for those assignments.

Although it has been demonstrated that many-body quasiparticle and excitonic effects are crucial for the correct description of the photoexcited states and for a quantitative understanding of such optical measurements [11], the single-particle gap is still a fundamental quantity because (i) it is the starting point for more elaborate descriptions and (ii) trends in the single-particle gap are often preserved by such refinements. Therefore, this work is devoted to describing the temperature dependence of the single-particle band gap of semiconducting SWNTs. From the calculated results for 18 different SWNTs, a complex dependence of $E_g(T)$ on chirality and diameter is found, with an unusual *nonmonotonic* behavior for certain classes of tubes. This behavior arises from the differences in sign of the e-p coupling associated with low-energy optical phonons. A model relation describing $E_g(T)$ for any given SWNT, as a function of diameter and chirality, is proposed.

The temperature dependence of E_g at constant pressure can be separated into harmonic and anharmonic contributions: $(\partial E_g/\partial T)_P = (\partial E_g/\partial T)_{\text{har}} + (\partial E_g/\partial T)_{\text{anh}}$. The harmonic term arises from the e-p interaction evaluated at the ground-state geometry. The anharmonic term is due to thermal expansion. The harmonic term is usually the more difficult one to evaluate and it has challenged theorists for many years [12–16]. We follow closely the formulation of Allen, Heine, and Cardona [14–16] to calculate $E_g(T)$ for semiconducting SWNTs. In the spirit of the adiabatic approximation [14], we write the shift of an electronic eigenenergy $\Delta E_{n,\mathbf{k}}$ of band n and wave vector $\mathbf{k}$ due to static atomic displacements from equilibrium as a second-order Taylor expansion:

$$\Delta E_{n,\mathbf{k}} = \mathbf{u} \cdot \nabla E_{n,\mathrm{k}} + \tfrac{1}{2}\mathbf{u} \cdot \mathbf{D} \cdot \mathbf{u}, \qquad (1)$$

where $\mathbf{u}$ is a $3N$-coordinate displacement vector and $\mathbf{D}$ is the corresponding $(3N \times 3N)$ Hessian matrix (N is the number of atoms). As usual, we express the displacements as a sum over normal modes [17]:

$$u(\alpha, \kappa) = \sum_j \left(\frac{\hbar}{2M_\kappa \omega_j}\right)^{1/2} \varepsilon_j(\alpha, \kappa)(a_j^\dagger + a_j), \qquad (2)$$

where $u(\alpha, \kappa)$ is the displacement along direction α of atom κ in the unit cell, with mass M_κ. The electron-phonon couplings will be directly evaluated using the "frozen-phonon" scheme [18]; therefore, the sum runs over zone-center modes j only, with frequency ω_j. In this approach, a sufficiently large supercell (equivalent to a fine Brillouin zone sampling) will be needed to achieve convergence. The $a_j^\dagger$ and a_j are creation and destruction operators for

phonons, and $\varepsilon_j(\alpha, \kappa)$ are components of the properly normalized polarization vectors.

We now substitute Eq. (2) into Eq. (1) and perform a thermal average [17]. In the harmonic approximation, the linear term in $\mathbf{u}$ vanishes and the final result is analogous to that in Ref. [15]:

$$\Delta E_{n,\mathbf{k}} = \sum_j \frac{\partial E_{n,\mathbf{k}}}{\partial n_j}\left(n_j + \frac{1}{2}\right), \tag{3}$$

where $n_j = (e^{\beta\hbar\omega j} - 1)^{-1}$ is the Bose-Einstein occupation number of the phonon mode j and the e-p coupling coefficient $\partial E_{n,\mathbf{k}}/\partial n_j$ is given by

$$\frac{\partial E_{n,\mathbf{k}}}{\partial n_j} = \frac{1}{2}\mathbf{x}_j \cdot \mathbf{D} \cdot \mathbf{x}_j, \tag{4}$$

where $x_j(\alpha, \kappa) = (\hbar/M_\kappa\omega_j)^{1/2}\varepsilon_j(\alpha, \kappa)$ are frozen-phonon displacements. From Eq. (1), this is simply the quadratic contribution to $\Delta E_{n,\mathbf{k}}$ when the atoms are displaced along a certain frozen-phonon $\mathbf{x}_j$. So, in practice, $\partial E_{n,\mathbf{k}}/\partial n_j$ is calculated by performing electronic structure calculations for $\pm\mathbf{x}_j$ and by averaging the obtained energy shifts so as to eliminate the linear term.

Structural relaxations and phonon calculations are performed using the extended Tersoff-Brenner interatomic potential [19]. Electronic structure is calculated using a multiple-neighbor, nonorthogonal tight-binding method [20,21]. Calculations are performed for 18 different semiconducting SWNTs with diameters $d = 7.6$–13.5 Å and spanning the entire range of chiralities: (6, 5), (7, 5), (7, 6), (8, 6), (8, 3), (8, 4), (9, 4), (9, 5), (9, 1), (11, 1), (10, 2), (12, 2), (10, 0), (11, 0), (13, 0), (14, 0), (16, 0), and (17, 0) [22].

Figure 1 shows the calculated (dots) values of $\Delta E_g(T) = E_g(T) - E_g(0)$ for all the 18 SWNTs studied. The lines are best fits to our model relation of Eq. (6), to be discussed below. For clarity, results are grouped into four panels according to similar values of the chiral angle θ. The temperature dependence of the band gap is relatively small compared to bulk semiconductors: From the set of calculated SWNTs, the largest value of $E_g(0) - E_g(300\ \mathrm{K})$ is 12 meV for the (16, 0) tube, with $(dE_g/dT)_{300\ \mathrm{K}} = -5.2 \times 10^{-2}$ meV/K. A strong and apparently complicated chirality and diameter dependence emerges: SWNTs with $\nu = (n - m)\mathrm{mod}3 = 2$ (solid dots) have, in general, smaller gap shifts than $\nu = 1$ tubes (open dots). Most interestingly, some $\nu = 2$ SWNTs with small chiral angles show a *nonmonotonic* gap variation with temperature that is positive for small T and negative for larger T. Some of these trends, in particular, the overall magnitude of the shifts and their ν oscillations, are observed in recent photoluminescence measurements in suspended SWNTs [24].

It is challenging to explain this interesting and complex behavior within a unified framework. The first step is to analyze the contributions to $E_g(T)$ from the different phonon modes. This information is contained in the e-p spectral function for the gap, g^2F, defined as [15]

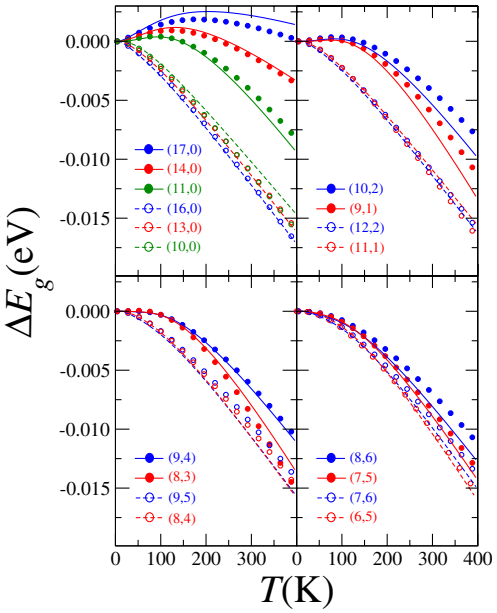

FIG. 1 (color online). Calculated and fitted $E_g(T)$. Solid dots and lines correspond to $\nu = 2$ SWNTs, whereas open dots and dashed lines correspond to $\nu = 1$ SWNTs.

$$g^2F(\Omega) = \sum_j \frac{\partial E_g}{\partial n_j}\delta(\Omega - \omega_j). \tag{5}$$

Note that $\partial E_g/\partial n_j$, defined as the difference between coupling coefficients for the two band-edge state [from Eq. (4)], can be positive or negative.

In Figs. 2(a) and 2(b) (lower panels) we plot g^2F for the (10, 0) and (11, 0) SWNTs, which are prototype examples of $\nu = 1$ and $\nu = 2$ tubes, respectively. The plots are restricted to the low-energy phonon branches (shown in the upper panels), the relevant ones to describe $E_g(T)$ for $T < 400$ K. We notice the g^2F (solid black line) is highly structured, reflecting the complexity of the phonon dispersion of these materials, even at low energies. In particular, we find that the low-energy optical "shape-deformation" modes (SDMs) near Γ provide the most important contributions to g^2F at low energies, shown by the red dashed lines. This family of modes is derived, in a zone-folding scheme, from the out-of-plane transverse-acoustical (ZA) branch of graphene and they deform the circular cross section of the tubes into a sequence of shapes: ellipse (the so-called "squashing mode"), triangle, square, pentagon, etc. For the (10, 0) tube, the contribution to g^2F from these modes is strongly negative and dominates the full g^2F up to phonon energies equivalent to 500 K. For the (11, 0) tube, this contribution is positive and smaller, but still dominates g^2F for $T < 200$ K. Beyond that temperature, the negative contributions from other modes start to become important. This competition explains the nonmonotonic behavior and smaller magnitudes of $E_g(T)$ shifts for $\nu = 2$ SWNTs.

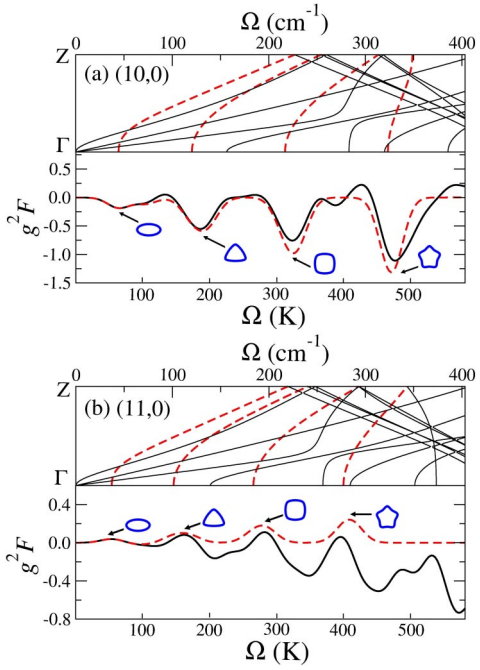

FIG. 2 (color online). Dimensionless g^2F (lower panels) and phonon spectra (upper panels) for (a) (10, 0) and (b) (11, 0) SWNTs. Lower panels: Solid black lines are the total g^2F and red dashed lines are the contributions from the shape-deformation modes (SDMs) near Γ. The g^2F is obtained from Gaussian broadening ($\sigma = 23$ K) of individual phonon contributions. Shapes for each SDM are also shown in the figure. Upper panels: Phonon frequencies (Ω) measured in both cm^{-1} and K. SDM branches are highlighted by red dashed lines.

Approximate model relations for $E_g(T)$ are common in semiconductor physics [25]. Despite not being exact, they are useful tools for a quick assessment of $E_g(T)$ for a given material. We propose a model relation for $E_g(T)$ of semiconducting SWNTs in the temperature range of $T < 400$ K as a two-phonon Viña model [26]:

$$\Delta E_g(T) = \frac{\alpha_1 \Theta_1}{e^{\Theta_1/T} - 1} + \frac{\alpha_2 \Theta_2}{e^{\Theta_2/T} - 1}, \tag{6}$$

where Θ_1 and Θ_2 ($\Theta_1 < \Theta_2$) are effective temperatures for the two "average phonons" and $\alpha_j \Theta_j = \partial E_g / \partial n_j$ are their effective e-p coupling coefficients. The resulting fits are shown in Fig. 1 as solid ($\nu = 2$) and dashed ($\nu = 1$) lines. Note that this model is equivalent to replacing the highly structured spectral functions shown in Fig. 2 by only two delta functions for each tube. Therefore, the resulting fits will necessarily be approximate. Nonetheless, as we see from Fig. 1, the largest deviation from numerical and model results is only 2 meV in the whole $T < 400$ K range. More importantly, as we shall see below, we are able to obtain a completely coherent and physically justified dependence of the parameters α_j and Θ_j on the SWNT's diameter and chirality.

We start by considering the parameter Θ_1, the effective frequency for the lowest-energy phonon modes. These modes dictate the low-temperature ($T \lesssim 100$ K) behavior of $E_g(T)$. These are the SDMs derived from the ZA branch of graphene. In graphene, this branch has a quadratic dispersion at low energies and momenta. Therefore, within a zone-folding description, we propose that the energies of these modes (and therefore Θ_1) should scale as the inverse square of the nanotube diameter d (in dimensionless units, $d = \sqrt{n^2 + m^2 + nm}$):

$$\Theta_1 = \frac{A}{d^2}. \tag{7}$$

Therefore, Θ_1 depends only on diameter and not on chirality.

The remaining parameters (α_1, Θ_2, and α_2) depend on chirality. The task of finding this dependence is enormously facilitated by the following ansatz: Dependence on chirality can be expressed as polynomial expansions $f(\xi)$ of a "chirality variable" $\xi = (-1)^\nu \cos(3\theta)$. This ansatz is reminiscent of trigonal warping effects in graphite [27,28] and is justified *a posteriori* by our numerical results. We consider up to second-order terms:

$$f_\eta(\xi) = \gamma_1^\eta \xi + \gamma_2^\eta \xi^2, \tag{8}$$

where η defines the parameter under consideration.

The parameter α_1 deserves special attention because it must embody the intriguing sign dependence of g^2F on ν for the SDMs described above. We find the following relation:

$$\alpha_1 = \alpha_1^0 + f_{\alpha_1}(\xi) d. \tag{9}$$

The derivation of this result involves a fascinating connection between dynamical and static radial deformations and will be presented elsewhere [29]. Similar "family behavior" [28] and sign oscillations with ν occur for static deformations induced by hydrostatic pressure [29] and uniaxial stress [30].

We now turn to the chirality and diameter dependence of α_2 and Θ_2. These parameters effectively represent a large number of phonon modes that start to become "active" at somewhat higher temperatures (between 350 and 500 K). In this energy range, the phonon density of states starts to become substantial, and we should expect that characteristics of particular nanotubes (chirality dependence) should gradually disappear and give rise to universal, graphitelike features. Of course, this is exact only in the limit of large d; therefore, for the relatively narrow tubes considered here, it is wise to include some chirality dependence [in the form of Eq. (8)] that decays with increasing diameter. We therefore propose the following expressions:

$$\Theta_2 = \Theta_2^\infty + \frac{f_{\Theta_2}(\xi)}{d}, \tag{10}$$

$$\alpha_2 = \frac{1}{d}\left(B + \frac{f_{\alpha_2}(\xi)}{d}\right). \tag{11}$$

The overall $1/d$ factor in α_2 is simple to understand, since $\alpha_1 + \alpha_2 = \lim_{T\to\infty} \frac{dE_g}{dT}$; i.e., α_2 is the graphitelike contri-

bution to the limiting slope of $E_g(T)$. We expect the high-temperature renormalization of the graphite bands around the Fermi point to be simply a rescaling of the Fermi velocity. Since the semiconducting SWNT gaps are obtained, in a simplified view, by slicing the band structure of graphene, we expect the corresponding change in the gap to be proportional to the gap itself, i.e., to $1/d$.

Equations (6)–(11) provide a ready-to-use recipe for estimating gap shifts with temperature for any nanotube in this diameter range [31]. The ten parameters are obtained by best fits: $A = 9.45 \times 10^3$ K, $\alpha_1^0 = -1.70 \times 10^{-5}$ eV/K, $\gamma_1^{\alpha_1} = 1.68 \times 10^{-6}$ eV/K, $\gamma_2^{\alpha_1} = 6.47 \times 10^{-7}$ eV/K, $\Theta_2^{\infty} = 470$ K, $\gamma_1^{\Theta_2} = 1.06 \times 10^3$ K, $\gamma_2^{\Theta_2} = -5.94 \times 10^{-2}$ K, $B = -4.54 \times 10^{-4}$ eV/K, $\gamma_1^{\alpha_2} = -2.68 \times 10^{-3}$ eV/K, and $\gamma_2^{\alpha_2} = -2.23 \times 10^{-5}$ eV/K.

Finally, we address the effects of thermal expansion in $E_g(T)$. Available descriptions of thermal expansion of isolated SWNTs seem to be controversial [32,33]. We propose that, for low-dimensional structures, one should describe thermal expansion effects in the band gap in terms of anharmonic changes of internal coordinates (bond lengths and angles), rather than lattice constants. The C-C bond changes quite similarly in all carbon structures (including diamond), although the lattice constants may behave quite differently [34]. Therefore, we use the well-established experimental data for the thermal expansion of diamond [35], where the thermal expansion of the lattice mirrors closely the thermal expansion of the bond, to estimate the gap shifts due to anharmonic effects. This leads to very small corrections in our calculated $E_g(T)$ values. For instance, the additional gap shift at 300 K for a (10, 0) tube due to anharmonic effects is only -0.2 meV. Therefore, we can safely neglect these effects in comparison with the harmonic contributions.

In conclusion, the calculated temperature dependence of the band gap of semiconducting carbon nanotubes shows a complex but systematic diameter and chirality dependence. Most gap shifts at 300 K are negative and small (less than 12 meV) with respect to 0 K. Therefore, temperature effects should not interfere with (n, m) assignments. Tubes with $\nu = 1$ have generally larger shifts than $\nu = 2$ tubes, and some $\nu = 2$ tubes with small chiral angles even display a nonmonotonic $E_g(T)$ curve. All these features are explained and reproduced by a two-phonon model relation, with diameter- and chirality-dependent parameters.

We acknowledge useful discussions with S. Saito, A. Jorio, R. B. Weisman, J. Wu, P. B. Allen, J. Lefebvre, P. Schelling, and Y.-K. Kwon. R. B. C. acknowledges financial support from the John Simon Guggenheim Memorial Foundation and Brazilian funding agencies CNPq, FAPERJ, Instituto de Nanociências, FUJB-UFRJ, and PRONEX-MCT. Work partially supported by NSF Grant No. DMR00-87088 and DOE Contract No. DE-AC03-76SF00098. Computational resources were provided by NPACI and NERSC.

[1] M. Becker and H. Y. Fan, Phys. Rev. **76**, 1531 (1949).
[2] O. Madelung, *Semiconductors: Group IV Elements and III-V Compounds* (Springer-Verlag, Berlin, 1991).
[3] M. Cardona *et al.*, Phys. Rev. Lett. **92**, 196403 (2004).
[4] S. Iijima, Nature (London) **354**, 56 (1991).
[5] A. Jorio *et al.*, Phys. Rev. Lett. **86**, 1118 (2001).
[6] Z. M. Li *et al.*, Phys. Rev. Lett. **87**, 127401 (2001).
[7] M. J. O'Connell *et al.*, Science **297**, 593 (2002).
[8] S. M. Bachilo *et al.*, Science **298**, 2361 (2002).
[9] A. Hartschuh *et al.*, Science **301**, 1354 (2003).
[10] J. Lefebvre *et al.*, Phys. Rev. Lett. **90**, 217401 (2003).
[11] C. D. Spataru *et al.*, Phys. Rev. Lett. **92**, 077402 (2004).
[12] H. Y. Fan, Phys. Rev. **82**, 900 (1951).
[13] E. Antončik, Czech. J. Phys. **5**, 449 (1955).
[14] P. B. Allen and V. Heine, J. Phys. C **9**, 2305 (1976).
[15] P. B. Allen and M. Cardona, Phys. Rev. B **23**, 1495 (1981).
[16] P. B. Allen and M. Cardona, Phys. Rev. B **27**, 4760 (1983).
[17] A. A. Maradudin, in *Dynamical Properties of Solids*, edited by G. K. Horton and A. A. Maradudin (North-Holland, Amsterdam, 1974), Vol. 1, p. 1.
[18] P. K. Lam and M. L. Cohen, Phys. Rev. B **25**, 6139 (1982).
[19] D. W. Brenner *et al.*, J. Phys. Condens. Matter **14**, 783 (2002).
[20] N. Hamada *et al.*, Phys. Rev. Lett. **68**, 1579 (1992).
[21] S. Okada and S. Saito, J. Phys. Soc. Jpn. **64**, 2100 (1995).
[22] We use six-unit supercells for zigzag tubes, which is enough to converge the gap shifts to within 0.1 meV in the 0 to 400 K range. Most chiral tubes already have a very long unit cell, therefore it is sufficient to consider just one-unit cell. Also, we have verified, for the (10, 0) and (11, 0) tubes, that our empirical description of the most relevant (low frequency) phonon frequencies and corresponding e-p couplings compare well (within $\sim$10% and $\sim$20%, respectively) with those calculated within first-principle methods using the SIESTA code [23].
[23] J. M. Soler *et al.*, J. Phys. Condens. Matter **14**, 2745 (2002).
[24] J. Lefebvre *et al.*, Phys. Rev. B **70**, 045419 (2004).
[25] R. Pässler, Phys. Status Solidi (b) **236**, 710 (2003).
[26] L. Viña *et al.*, Phys. Rev. B **30**, 1979 (1984).
[27] R. Saito *et al.*, Phys. Rev. B **61**, 2981 (2000).
[28] S. Reich and C. Thomsen, Phys. Rev. B **62**, 4273 (2000).
[29] R. B. Capaz, C. D. Spataru, P. Tangney, M. L. Cohen, and S. G. Louie (to be published).
[30] Y. N. Gartstein *et al.*, Phys. Rev. B **68**, 115415 (2003).
[31] We have also calculated the temperature shifts for the second allowed transition (E_{22}). The results can be understood within the same framework as E_g (or E_{11}), provided that the diameter dependences of α_1 and α_2 are rescaled by a factor of 2 and the sign factor $(-1)^{\nu}$ is reversed.
[32] Y.-K. Kwon *et al.*, Phys. Rev. Lett. **92**, 015901 (2004).
[33] P. K. Schelling and P. Keblinski, Phys. Rev. B **68**, 035425 (2003).
[34] N. R. Raravikar *et al.*, Phys. Rev. B **66**, 235424 (2002).
[35] *American Institute of Physics Handbook*, edited by D. E. Gray (McGraw-Hill, New York, 1972), 3rd ed.